Velocity distributions in microskimmer supersonic expansion helium beams: High precision measurements and modeling

S. D. Eder, A. Salvador Palau, T. Kaltenbacher, G. Bracco, and B. Holst

Velocity distributions in microskimmer supersonic expansion helium beams: High precision measurements and modeling

S. D. Eder,[1,a),b)] A. Salvador Palau,[2,a)] T. Kaltenbacher,[1,a)] G. Bracco,[1,3] and B. Holst[1]

[1]*Department of Physics and Technology, University of Bergen, Allégaten 55, 5007 Bergen, Norway*
[2]*Department of Engineering, Institute for Manufacturing, University of Cambridge, Cambridge CB3 0FS, United Kingdom*
[3]*CNR-IMEM, Department of Physics, University of Genova, V Dodecaneso 33, 16146 Genova, Italy*

Supersonic molecular beams are used in many applications ranging from spectroscopy and matter wave optics to surface science. The experimental setup typically includes a conically shaped, collimating aperture, the skimmer. It has been reported that microskimmers with diameters below 10 μm produce beams with significantly broader velocity distributions (smaller speed ratios) than larger skimmers. Various explanations for this phenomenon have been proposed, but up till now, only a limited amount of data has been available. Here we present a systematic study of the velocity distribution in microskimmer supersonic expansion helium beams. We compare a 4 μm diameter skimmer with a 390 μm diameter skimmer for room temperature and cooled beams in the pressure range 11-181 bars. Our measurements show that for properly aligned skimmers, the only difference is that the most probable velocity for a given pressure and temperature is slightly lower for a microskimmed beam. We ascribed this to the comparatively narrow and long geometry of the microskimmers which can lead to local pressure variations along the skimmer channel. We compare our measurements to a model for the supersonic expansion and obtain good agreement between the experiments and simulations. *Published by AIP Publishing.* https://doi.org/10.1063/1.5044203

I. INTRODUCTION

Supersonic molecular beams are used in a range of scientific disciplines. Helium beams, in particular, are an established tool in surface science used in diffraction experiments and dynamics studies (diffusion and surface vibrations) and for monitoring thin film growth and thermal evaporation.[1,2] Work is ongoing to extend the use of helium beams toward direct imaging in neutral helium microscopes.[3–7] Molecular beams can also be employed as a carrier gas for deposition of other molecules.[8]

A supersonic molecular beam is created by a supersonic (free jet) expansion: atoms or molecules from a high pressure reservoir (typically up to 200 bars or more) expand into vacuum through a nozzle with a diameter larger than the mean free path of the gas particles in the reservoir. The expansion is adiabatic. As the atoms or molecules expand into vacuum, they collide until free molecular flow is reached. The advantage of the supersonic expansion compared to an effusive beam is the high beam density and narrow velocity distribution that can be achieved.[9] The central part of the beam is selected by a conically shaped, circular aperture, popularly referred to as the skimmer.

For most experiments, the skimmer has a diameter between 200 μm and a few mm. The first experiments using a microskimmer were presented by Braun *et al.*[10] This paper introduces the method of glass pulling for the creation of microskimmers which is used to this day. Measurements were obtained using a source pressure of 120 bars and a 10 μm diameter nozzle. In the paper, it is reported that speed ratios for 3 μm and 5 μm skimmers are considerably lower than those for a standard 1.6 mm diameter skimmer: 65 and 24, respectively, compared to 78 for the standard skimmer. The speed ratio is a standard way to express the quality of a molecular beam and is defined as $2\sqrt{\ln 2}\, u/\Delta u$ where u is the most probable (mean) velocity and Δu is the full width at half maximum (FWHM) of the velocity distribution.[11,12]

Braun *et al.* proposed geometrical imperfections and/or imperfections of the lip edge of the skimmer as well as difficulties in aligning the skimmer and nozzle as possible explanations for the reduced speed ratios. In their paper, they suggested that microskimmers can be used for atom optics experiments and indeed up till now, this has been the main application. The first experiment using a microskimmer to focus a neutral helium beam was carried out by Doak *et al.*[13] Focusing measurements were carried out using skimmers between 1 μm and 14 μm in diameter with a source pressure up to 150 bars and a 5 μm diameter nozzle. The expected focused spot diameter was not achieved. The relative deviation between expected and measured focus increases from 1.1 for a 14 μm skimmer (5.6 μm expected, 6.2 μm measured) to 5 (0.4 μm expected, 2 μm measured) for the 1 μm skimmer. It is suggested in the paper that this is due to the supersonic expansion continuing after the beam has passed through the skimmer aperture. It is stated that measurements were carried out for velocity distributions $\Delta u/u$ between ~1% FWHM and up to ~10% FWHM (corresponding to speed ratios between around 140 and 14). These speed ratios are not compared explicitly to standard

skimmer measurements. The first neutral helium microscopy images were obtained a few years later. The resolution was around 2 μm, using a 1.2 μm diameter skimmer.[3] Experiments were also carried out with a 2.4 μm diameter skimmer. The paper states that speed ratios between 16 ± 1 and 140 ± 3 were obtained with source pressures between 11 bars and 191 bars using a 10 μm diameter nozzle. The paper also states that chromatic aberrations caused by the velocity distribution of the beam are the resolution limiting factor and that no signs of further expansion after the beam has passed through the skimmer could be observed. The first sub-micrometer focusing was obtained by Eder *et al.*[4] A microskimmer 1.1 μm in diameter was used. The measurements were performed at a source pressure of 81 bars and 110 bars using a 10 μm nozzle. However, the velocity distributions were not measured explicitly; instead, theoretical values were used to calculate the expected focus size. The agreement between the theoretically expected (calculated) and measured focus spot diameters was good, but the measurements had large error bars (up to ±34% of the measured focus spot diameter).

The importance of the speed ratio for the microscope resolution is discussed in Ref. 14. As described in detail in Ref. 14, the diffractive beam focusing elements used in some helium microscopes have chromatic aberrations. In order to achieve high resolution (small focus diameters) with such microscopes, the source, i.e., the skimmer diameter, needs to be as small as possible and at the same time the beam as monochromatic as possible. A lower speed ratio will lead to a lower resolution. This together with the discussion above illustrates how important it is to determine the true, best obtainable velocity distribution from microskimmers. In this paper, we present such a detailed study. Of particular importance is the use of our molecular beam source which allows the skimmer to be positioned with sub-micrometer precision relative to the nozzle.[15] Microskimmer measurements are compared with measurements using a standard skimmer. To ensure accurate measurements of high speed ratios, we employ our improved time-of-flight (TOF) method presented in Ref. 16. Further we use our theoretical model for the supersonic expansion described in Refs. 17 and 18 to model the experimental data. The model is described in Sec. III.

II. EXPERIMENTAL SETUP

The experiments presented here were carried out in the molecular beam apparatus at the University of Bergen, popularly referred to as MAGIE.[19] A drawing of the experimental setup can be seen in Fig. 1.

The neutral helium beam was created by a free jet expansion from a source reservoir through a 10 ± 1 μm diameter nozzle (Plano GmbH, A0300P). The central part of the beam was selected by either a standard skimmer (Beam Dynamics, Inc.) with a diameter of 390 μm or with a self-made glass microskimmer with a diameter of 4 μm. The microskimmer was made using a commercial micropipette puller (Narishige, PP-830) and lead glass tubes (Corning 8161) with an outer diameter of 1.5 mm and an inner diameter of 1.1 mm. The
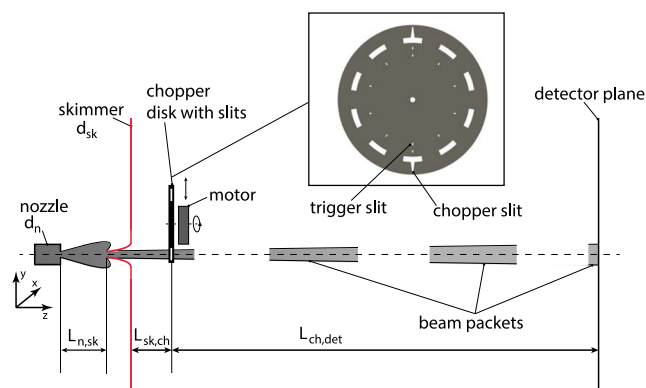

FIG. 1. Schematic representation of the TOF measurement setup. Inset: Detailed drawing of the chopper disk with its two trapezoidal shaped slits placed 180° apart. The trigger slits are used to tag each beam packet. Further details are given in the text.

key challenge when pulling microskimmers is to achieve the right skimmer opening angle even for small apertures. Bird described the expected quality differences between the flow in slender or wide angle skimmers.[20] Slender skimmers with opening angles below ~35° are predicted to give better skimming performance than wide angle skimmers. But as the skimmer becomes more slender, beam attenuation will occur due to collisions with molecules reflected from the skimmers' internal wall. Eventually this will lead to a break down of the beam. A break down of the beam is a rapid transition from supersonic to subsonic beam flow which is often described as a sudden blocking of the skimmer. Due to the somewhat manual nature of the skimmer pulling procedure, it is difficult to reproduce exactly the same openings and angles for individual skimmers. Generally the best skimmers were obtained by using a relatively high heating setting (70), high pulling force (about 100 g), and several heating steps (6). Decreasing the temperature or decreasing the number of heating steps made the taper of the skimmer longer and hence the opening angle smaller. Figure 2 shows a stereo microscope image (a) and a scanning electron microscope (SEM) image (b) of our self-made skimmer. The outer skimmer opening angle was determined from the stereo microscope image in Fig. 2(a) and found to be ~32.5° for the first ca. 200 μm followed by a more narrow section of ~12.5° opening angle. The microskimmer opening is circular [see Fig. 2(b)] with the opening lips having an estimated thickness of less than ~200 nm. After pulling, the glass tube was glued onto a copper holder using a two component glue (UHU PLUS ENDFEST 300). The length of the skimmer's glass tip protruding out of the copper holder was approximately 2.5 mm. After the glue had hardened, the glass tube was cut as short as possible to the inner rim of the copper holder using a diamond knife to just leave the top part. The mounting was performed using a stereo microscope. Care was taken to ensure that the skimmer opening was parallel to the mounting base so that the beam and skimmer opening were perpendicular to each other.

For all experiments, the skimmer was placed 11.5 ± 0.5 mm in front of the nozzle ($L_{n,sk}$). The distance from skimmer to chopper was 525 ± 1 mm ($L_{sk,ch}$), and the distance from chopper to detector was 1905 ± 5 mm ($L_{ch,det}$).

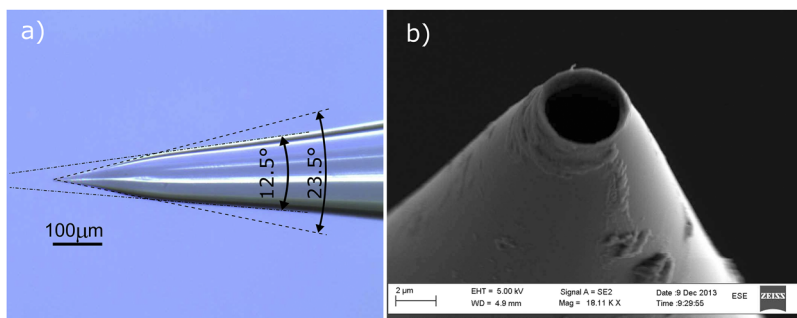FIG. 2. (a) Stereo microscope image of the ∅ 4 μm microskimmer (glass). (b) SEM image of the ∅ 4 μm microskimmer (glass).

The beam source in MAGIE has been specifically designed for microskimmer experiments and is to our knowledge the only molecular beam source which allows positioning of the skimmer relative to the nozzle with sub-micrometer precision.[15] The source was operated at pressures in the range 11-181 bars at two different source temperatures, nominally 300 K and 125 K, obtained by cooling the nozzle with liquid nitrogen. For the alignment of the nozzle relative to the microskimmer, the nozzle is moved in the x and y directions across the skimmer opening (see Fig. 1). The optimum nozzle to skimmer position is found when the detected beam signal reaches a maximum. The detailed alignment procedure can be found in Ref. 15. It should be noted that the effective ionization area of the MAGIE detector is large: 4.6 × 6.6 mm. Thus, even though a skimmer exchange might slightly vary the detector entrance position of the investigated He beam, the described alignment procedure in combination with the relatively big size of the detector entrance ensures a sampling of the beams' centerline. The fixed skimmer to detector position for each investigated skimmer also ensures that the angle of the beam within the
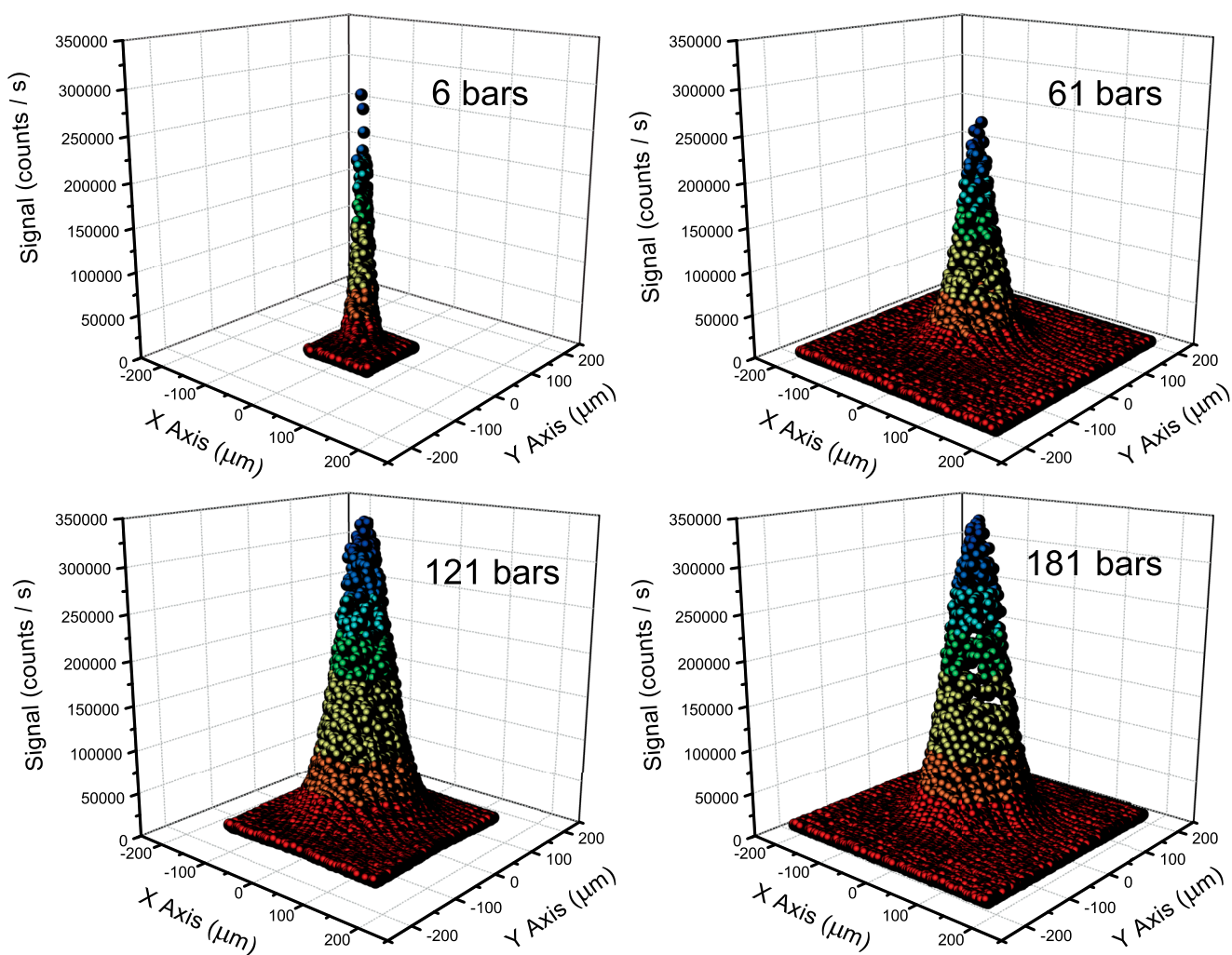

FIG. 3. 2D intensity maps recorded by scanning the 10 μm nozzle over the 4 μm glass skimmer (RT beam). Since the glass skimmer diameter is small compared to the spatial extension of the supersonic expansion, this 2D intensity maps can be seen as an approximate image of the expansion itself.

skimmer is constant for all different skimmers since the nozzle position is optimized for each measurement set. Possible small variations of the detector efficiency depending on where the beam enters the detector are not an issue for the presented measurements since the detector efficiency only affects the count rate not the TOF distribution. Figure 3 shows a recorded 2D x/y scan intensity map for the alignment of the nozzle with the 4 μm diameter microskimmer for 4 different source pressure values at 300 K. As can be seen in Fig. 3, the spatial extension of the 2D source profile increases with increasing source pressure values. This corresponds well to the theoretically expected and experimentally verified behavior of a spatial increase in the free jet expansion with pressure.[17,18,21,22] A higher source pressure leads to an increase in the detected source intensity likewise agreeing well with theoretical considerations.

The most probable beam velocity and the beam velocity distribution were obtained by time of flight measurements (TOF). The beam was chopped by a mechanical chopper operated at frequencies of 230 Hz, 310 Hz, and 320 Hz. The chopper is linked to a light emitting diode (LED)-photodetector system which sends a trigger signal to the detector electronics so that the arrival time for the atoms in each beam pulse is recorded. The TOF signal is determined by the actual velocity distribution of the beam convoluted with the chopper slit and the detector function. When the velocity distribution is narrow (speed ratio high), it cannot be determined accurately using the standard deconvolution procedure described in Ref. 12. We therefore used a new method recently developed in our group which allows the velocity distribution to be extracted with high accuracy.[16] The improved method is based on a systematic variation of the chopper convolution parameters providing a set of independent measurements that can be fitted to obtain the helium beams speed ratio.

III. THEORETICAL MODEL

Our theoretical model for the supersonic helium expansion is based on a theory proposed by Toennies and Winkelmann[23] in which the solution of the Boltzmann equation is obtained by means of the method of moments and assuming a Lennard-Jones (LJ) potential for the He-He interaction. The model was extended by Pedemonte *et al.*[24] to include other analytical He-He potentials, in particular the Hurly Moldover (HM) potential.[25] As in a previous study,[18] the calculations presented were performed treating helium as a real gas and employing the equation of state obtained by McCarty.[26]

The first assumption is to treat the expansion as spherically symmetric. Then an ellipsoidal velocity distribution (f_{ell}), which consists of two Maxwell distributions parameterized by two different temperatures (denoted by $T_{||}$ and $T_{\perp}$ for the parallel and the perpendicular velocity components with respect to streamlines) is introduced,

$$f_{ell}(\vec{v}) = n \Big(\frac{m}{2\pi k_b T_{||}} \Big)^{\frac{1}{2}} \Big(\frac{m}{2\pi k_b T_{\perp}} \Big)$$
$$\times \exp \Big(-\frac{m}{2k_b T_{||}} (v_{||} - u)^2 - \frac{m}{2k_b T_{\perp}} v_{\perp}^2 \Big),$$

where m is the mass, n is the number density, $v_{||}$ and $v_{\perp}$ are the radial and perpendicular components of the velocity, and u is the most probable velocity of the expanding gas. The evolution of the parameters n, u, $T_{||}$, and $T_{\perp}$ with the distance from the source (z) is obtained by solving numerically the equations which contain the collision integral (2, 1),

$$\Omega^{(2,1)}(T_{eff}) = \Big(\frac{k_b T_{eff}}{\pi m} \Big)^{(1/2)} \int_0^\infty Q^{(2)}(E) \gamma^5 \exp(-\gamma^2) d\gamma,$$
$$\gamma = \sqrt{\frac{E}{k_b T_{eff}}}, \tag{1}$$

where T_{eff} is an effective average temperature varying between $T_{\perp}$ and $T_{||}$, $Q^{(2)}$ is the viscosity cross section, and E is the collision energy of two atoms in the center-of-mass system. For collisions between Bose-Einstein particles, the viscosity cross section is defined as

$$Q^{(2)}(E) = \frac{8\pi \hbar^2}{mE} \sum_{l=0,2,4,\dots} \frac{(l+1)(l+2)}{(2l+3)} \sin^2(\eta_{l+2} - \eta_l),$$

where η_l is the phase shift of the partial wave with orbital angular momentum l. For the present article, calculations were performed for LJ and HM potentials. Moreover, we have also considered the Pirani *et al.* (PI) potential[27,28] which modifies and improves the LJ potential ($V(r)$) retaining a simple expression

$$V(r) = \varepsilon \Big(\frac{\mu}{n(r) - \mu} \Big(\frac{r_m}{r} \Big)^{n(r)} - \frac{n(r)}{n(r) - \mu} \Big(\frac{r_m}{r} \Big)^{\mu} \Big),$$

where for He, $\mu = 6$, r is the distance, and $n(r)$ is given by

$$n(r) = \beta + 4 \Big(\frac{r}{r_m} \Big)^2,$$

with parameters $r_m = 2.974$ Å, $\beta = 8$, and $\varepsilon = 2.974$ meV.[29]

IV. RESULTS AND ANALYSIS

Figures 4(a) and 4(b) show measurements of the most probable velocity (maximum velocity of the distribution) for different pressures for a cold and a room temperature beam. As can be seen, the theory reproduces the general trend of the experiments although there is a systematic deviation at lower pressures (the nozzle size d_n was kept constant throughout the experiment). It is not quite clear what causes this deviation. From an instrument design point of view, the high pressure range, which gives the highest speed ratio, is the most important. We also note that the velocities for the microskimmed beams are slightly lower (up to around 1%) for a given pressure for both temperatures. The reason for this is not quite clear. However, even though a smaller skimmer has a higher Knudsen number K_n and thus is assumed to show less skimmer interferences (see Ref. 20), the comparatively long and narrow geometries of microskimmers can possibly cause local pressure variations along the skimmer channel and this may slow the beam down, i.e., through a funnelling effect. It is surprising though that the effect does not increase with the source pressure.

Figures 5(a) and 5(b) show the corresponding speed ratio plots for the two temperatures. The first thing to note is the
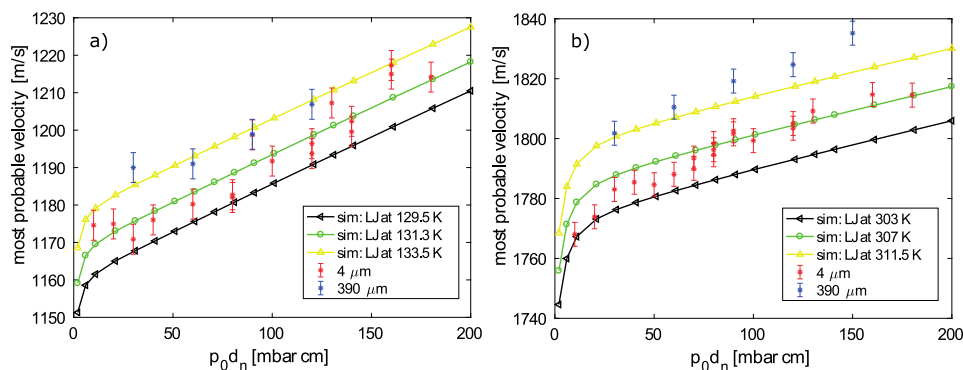
FIG. 4. Experimental results and simulations for the most probable velocity for cold beams (a) and for room temperature beams (b) as a function of $p_0 d_n$, where p_0 is the source reservoir pressure and d_n is the nozzle diameter. Note the slightly lower velocity for the microskimmer beam. This is discussed in the main text.

near to perfect overlap between the microskimmer and standard skimmer measurements. These results agree well with the prediction of Bird *et al.* stating that as long as the internal skimmer angle is greater than the effective angle of the thermal spreading of the beam, no significant collisions of molecules with the internal skimmer surface occur. Thus as

long as the speed ratio is sufficiently high to attain this condition, no major internal skimmer interferences are expected. Furthermore, there is a reasonable agreement between theory and experiments although it is interesting to see that for higher pressures, the simulations seem to predict too high speed ratios for the cold beam and too low speed ratios for
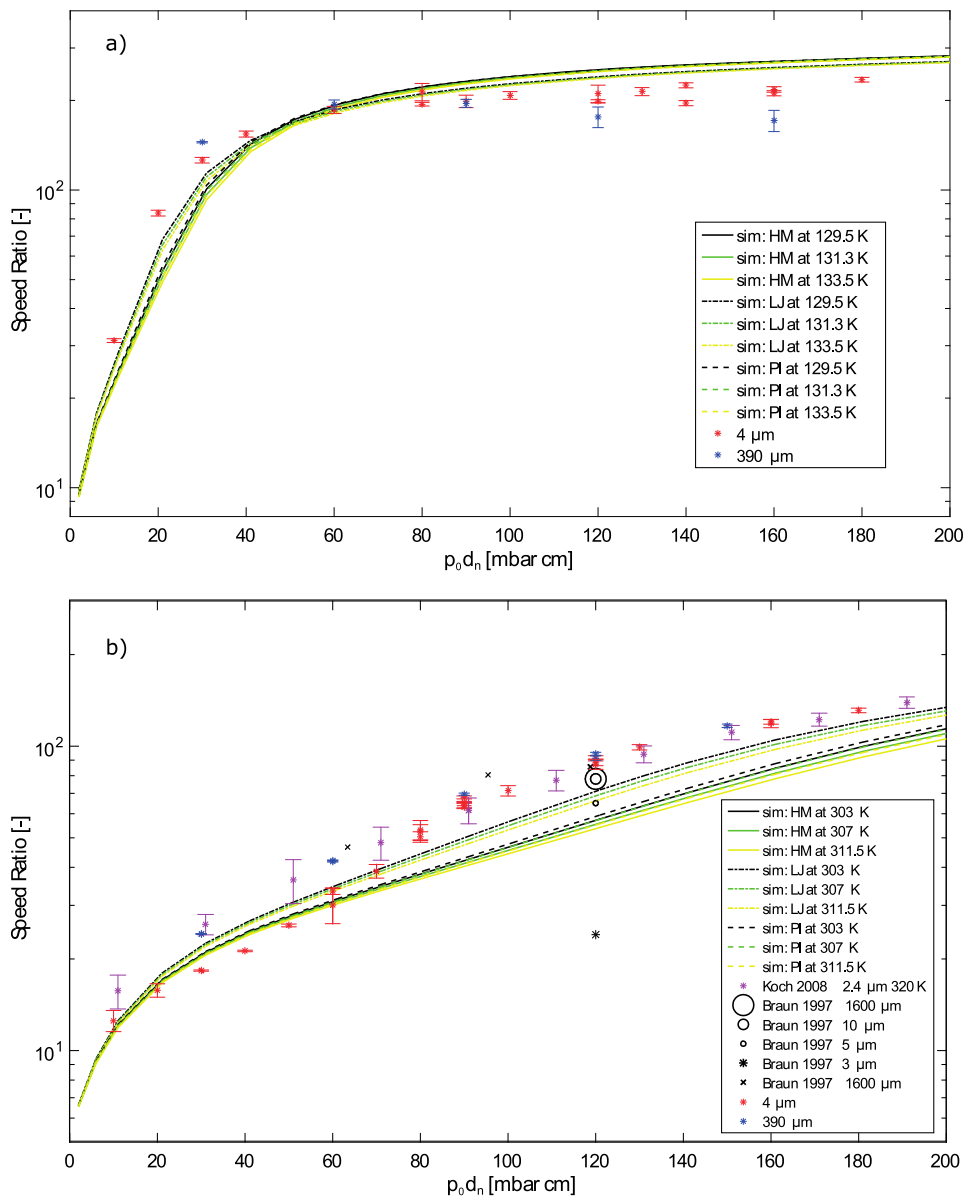

FIG. 5. Experimental results and simulations for the speed ratio of cold temperature beams (a) and room temperature beams (b) plotted together with simulations. For comparison, the speed ratio data from Braun *et al.*[10] and Koch *et al.*[3] are added to the room temperature plot in (b). Note the very similar behavior of microskimmer and standard skimmer as well as the very little variations in the results for the different simulations at different temperatures.

the warm beam. Comparing the three different potentials used for the simulation (LJ, HM, and PI), the LJ potential gives the best agreement for the present experimental conditions [most prominent for the room temperature beam, see Fig. 5(b)]. This better agreement of LJ potential was also observed in Ref. 25 for temperatures above 50 K or in Refs. 17 and 18. Finally, the strong disagreement between the presented 4 μm microskimmer measurements and the 3 μm microskimmer results from Braun *et al.* should be noted. Braun *et al.* proposed geometrical imperfections and/or imperfections of the lip edge of the skimmer as well as difficulties in aligning the skimmer and nozzle as possible explanations for the reduced speed ratios. A comparison between the skimmer images in Ref. 10 and Fig. 2 suggests that the skimmer geometries of both skimmers are similar. This leads us to the conclusion that most likely the mentioned misalignment is the reason for the reduced speed ratio experienced by Braun *et al.*

V. CONCLUSION

In this paper, we have presented a systematic study of velocity distributions of helium beams collimated by a microskimmer for a room temperature beam and a cooled beam. The measurements were carried out in the pressure range 11 bars–181 bars. Our results show that when the microskimmer is properly aligned with the nozzle, the speed ratio for the microskimmer does not differ from that of a standard skimmer. The most probable velocities for microskimmers appear to be slightly smaller than for standard skimmers. We measured a difference of up to around 1%. We attribute this to variations in the local pressure caused by the internal microskimmer geometry, i.e., a funnelling effect and/or scattering from the entrance interior lip, although the effect is not fully understood. Furthermore, we show that the experimental data fit well to the theoretical model we have developed.

[1] D. Farías and K.-H. Rieder, Rep. Prog. Phys. **61**, 1575 (1998).
[2] G. Bracco and B. Holst, *Surface Science Techniques* (Springer, 2013).
[3] M. Koch, S. Rehbein, G. Schmahl, T. Reisinger, G. Bracco, W. E. Ernst, and B. Holst, J. Microsc. **229**, 1 (2008).
[4] S. D. Eder, T. Reisinger, M. M. Greve, G. Bracco, and B. Holst, New J. Phys. **14**, 073014 (2012).
[5] P. Witham and E. Sanchez, Rev. Sci. Instrum. **82**, 103705 (2011).
[6] A. Fahy, M. Barr, J. Martens, and P. C. Dastoor, Rev. Sci. Instrum. **86**, 023704 (2015).
[7] M. Barr, A. Fahy, J. Martens, A. P. Jardine, D. J. Ward, J. Ellis, W. Allison, and P. C. Dastoor, Nat. Commun. **7**, 10189 (2016).
[8] L. Vattuone, G. Bracco, M. Smerieri, L. Savio, and M. Rocca, *Dynamics of Gas-Surface Interactions: Atomic-Level Understanding of Scattering Processes at Surfaces* (Springer, Heidelberg, New York, Dordrecht, London, 2013).
[9] G. Scoles, *Atomic and Molecular Beam Methods* (Oxford University Press, New York, Oxford, 1988).
[10] J. Braun, P. K. Day, J. P. Toennies, G. Witte, and E. Neher, Rev. Sci. Instrum. **68**, 3001 (1997).
[11] D. J. Auerbach, *Atomic and Molecular Beam Methods* (Oxford University Press, 1988).
[12] H. Pauly, *Atom, Molecule, and Cluster Beams 2* (Springer, 2000).
[13] R. B. Doak, R. E. Grisenti, S. Rehbein, G. Schmahl, J. P. Toennies, and C. Wöll, Phys. Rev. Lett. **83**, 4229 (1999).
[14] T. Reisinger and B. Holst, J. Vac. Sci. Technol., B: Microelectron. Nanometer Struct.–Process., Meas., Phenom. **26**(6), 2374 (2008).
[15] S. D. Eder, B. Samelin, G. Bracco, K. Ansperger, and B. Holst, Rev. Sci. Instrum. **84**, 093303 (2013).
[16] A. S. Palau, S. D. Eder, T. Kaltenbacher, B. Samelin, G. Bracco, and B. Holst, Rev. Sci. Instrum. **87**, 023102 (2016).
[17] T. Reisinger, G. Bracco, S. Rehbein, G. Schmahl, W. E. Ernst, and B. Holst, J. Phys. Chem. A **111**, 12620 (2007).
[18] S. D. Eder, G. Bracco, T. Kaltenbacher, and B. Holst, J. Phys. Chem. A **118**, 4 (2014).
[19] A. Apfolter, "Wiederaufbau und test einer He-streuapparatus und erste streuexperimente an amorpher sowie kristalliner SiO$_2$-oberflche," M.Sc. thesis, Graz University of Technology, 2005.
[20] G. A. Bird, Phys. Fluids **19**, 1486 (1976).
[21] T. Reisinger, M. M. Greve, S. D. Eder, G. Bracco, and B. Holst, Phys. Rev. A **86**, 043804 (2012).
[22] T. Nesse, S. D. Eder, T. Kaltenbacher, J. O. Grepstad, I. Simonsen, and B. Holst, Phys. Rev. A **95**, 063618 (2017).
[23] J. Toennies and K. Winkelmann, J. Chem. Phys. **66**, 3965 (1977).
[24] L. Pedemonte, G. Bracco, and R. Tatarek, Phys. Rev. A **59**, 3084 (1999).
[25] L. Pedemonte and G. Bracco, J. Chem. Phys. **119**, 1433 (2003).
[26] R. D. McCarty and V. D. Arp, "A new wide range equation of state for helium," in *Advances in Cryogenic Engineering* (Springer, Boston, MA, 1990).
[27] F. Pirani, M. Albertí, A. Castro, M. M. Teixidor, and D. Cappelletti, Chem. Phys. Lett. **394**, 37 (2004).
[28] F. Pirani, S. Brizi, L. F. Roncaratti, P. Casavecchia, D. Cappelletti, and F. Vecchiocattivi, Phys. Chem. Chem. Phys. **10**, 5489 (2008).
[29] S. Longo, P. Diomede, A. Laricchiuta, G. Colonna, M. Capitelli, D. Ascenzi, M. Scotoni, P. Tosi, and F. Pirani, in *Computational Science and Its Applications—ICCSA 2008*, edited by O. Gervasi, B. Murgante, A. Laganà, D. Taniar, Y. Mun, and M. L. Gavrilova (Springer, Berlin, Heidelberg, 2008).